Journal of Electroanalytical Chemistry 920 (2022) 116592

Contents lists available at ScienceDirect

Journal of Electroanalytical Chemistry

journal homepage: www.elsevier.com/locate/jelechem

Electrochemical and physicochemical degradability evaluation of printed flexible carbon electrodes in seawater

Fabiane F. Franco [a,*], Saoirse Dervin [b], Libu Manjakkal [c,d,*]

[a] Water and Environment Group, Infrastructure and Environment Division, James Watt School of Engineering, University of Glasgow, Glasgow G12 8LT, UK
[b] Merck Life Sciences, Glasgow, UK
[c] Electronic and Nanoscale Engineering, James Watt School of Engineering, University of Glasgow, Glasgow G12 8LT, UK
[d] School of Computing and Engineering & the Built Environment, Edinburgh Napier University, Merchiston Campus, EH10 5DT, UK

ARTICLE INFO

Keywords:
Screen Printing
Sustainable Flexible Carbon Electrodes
Physical and Chemical Degradability
Seawater monitoring
Electrochemical Studies

ABSTRACT

The environmental impact of metals and non-degradable plastics in printed electrodes has highlighted the need of employing sustainable materials in environmental monitoring. In this work, we developed a new sustainable graphite-based paste (G-PE) printed on a bioderived and biodegradable polyhydroxybutyrate polyhydroxyvalerate substrate for tap water and seawater monitoring. We compared its performance against two standard screen-printed electrodes (SPEs) fabricated using commercial silver and carbon pastes (Ag-SPEs and C-SPEs) printed on a polyvinyl chloride substrate. The Ag-SPEs exhibited the lowest sheet resistance (R_S = 0.053 Ω/sq), however they were also less reliable as silver oxidised and reacted with ions present in seawater. Meanwhile, the C-SPEs and G-PE presented similar R_S (26.9 and 30.1 Ω/sq, respectively), were inert in different media and showed relatively stable response during cyclic bending studies (less than 2.3% relative resistance variation for the C-SPE). Physical and chemical degradation studies of the sustainable G-PE in seawater demonstrated relatively quick ultrasound induced dissolution (less than5 min) while the SPEs did not dissolve even after 30 min of sonication, highlighting the suitability of this new, eco-friendly G-PE for single use or short-term water quality monitoring applications.

1. Introduction

Printed electrochemical devices have been attracting substantial attention over the past decades, becoming a well-established field. Their facile fabrication, cost-effectiveness and easy operation are some of the characteristics that allow these devices to operate in a range of different areas, such as energy storage, wearable sensors, and environmental monitoring [1–5]. With increasing usage and integration of sensors, it is desirable to have materials that are biodegradable and/or more sustainable to reduce the environmental impact, especially for single-use or disposable sensors. The use of non-degradable plastics and metals heavily impact the life cycle assessment of the electrode [6]. However, substitution of key components in printed electronics can negatively affect the electrode performance and stability, due to poor paste adhesion to the substrate and unexpected chemical reactions with the conductive electrode patch. These challenges become even more prominent in electrodes employed for water monitoring. Common sustainable substrate materials, such as paper, cotton, and jute, either dissolve too quickly or have a high water intake, making its integration in water difficult [7–9]. Furthermore, the investigation of potentially sustainable materials for the conductive pathway often does not account for other chemicals used in ink and paste preparation [6,10]. Other parts of sensor fabrication, such as the sensor disposability and the influence on the electrochemical measurements after integration of new conductive path/substrate materials, are often not investigated. In practical applications, it is important to conduct a thorough analysis of every component to reach a more sustainable production with reliable results. Therefore, a careful selection of materials for the substrate and the conductive path of disposable sensors that are economically feasible should be taken into consideration in the development of electrochemical devices.

In this regard, screen-printing is an affordable and versatile fabrication technique that allows sensors to be printed on flexible and rigid substrates [11]. Both flexible and rigid screen-printed sensors are commonly employed in routine environmental analysis, such as in pH, pesticide, heavy metal, bacteria, and inorganic nitrogen detection [3,12,13]. For these sensors, the sensitive material synthesis (e.g. metal oxides, graphite composite, carbon nanotubes, conductive poly-

* Corresponding authors.
E-mail addresses: Fabiane.Franco@glasgow.ac.uk (F.F. Franco), Libu.Manjakkal@glasgow.ac.uk (L. Manjakkal).

https://doi.org/10.1016/j.jelechem.2022.116592
Received 5 January 2022; Received in revised form 1 June 2022; Accepted 3 July 2022
Available online 6 July 2022

mers, etc.) and the different analyte detection methods (e.g. potentiometric, amperometric, chemi-resistive) are widely discussed in literature [2,12,13]. The conductive path in printed electrodes generally uses carbon, silver, gold, and platinum pastes [13]. Gold and platinum present many of the desirable characteristics of a good conductive path material, e.g., high stability in the desired working window, low electrical resistance, and inertness in the chosen chemical environment. However their high cost and disposability issues prevent their widespread use in printed sensors [13]. The metal of choice, in such cases, is silver, as it is highly conductive and affordable. Although more abundant and less harmful when compared to other precious metals, silver is not a long-term viable option as it still exhibits a high environmental impact [6]. Besides, silver is known to react with halides to form new components, and this has been thoroughly studied in literature in the form of chloride, iodine, and bromide sensors [14–16]. Silver can also react with sulphates to form $Ag/AgSO_4$, which has been used as an alternative to the Ag/AgCl reference electrode (RE) [17,18]. Considering that silver readily reacts with components present in water bodies (e.g., NaCl, $MgSO_4$), which could rapidly deteriorate the performance and the lifetime of the sensor, and its high environmental impact, other options for the conductive path material should be explored. A metal-free alternative is carbon, as it is an inexpensive, inert material with a broad potential window, although it is usually used in the active working electrode (WE) area and not on the entire conductive pathway due to its lower conductivity [13,19]. For electrochemical applications the carbon paste could be modified with graphene and carbon nanotubes (CNTs), for example [20–22]. Here, CNT was used to promote electron transfer reactions and enhance the stability of the printed electrodes [20]. However, to employ carbon paste electrodes as a conductive track it is essential to overcome the issue of high resistance. To further enhance the conductivity, the annealing temperature of the carbon additives and the binders also need to be investigated [23,24]. In one of the works, it was noted that to enhance the conductivity of printed carbon electrodes it is necessary to increase the size of the graphene flakes and minimize the amount of stabilizer used in the final ink formulation [23]. In another work, heat treatment was carried out to increase the conductivity by controlling the variation of the filter/matrix interaction and crystallisation of the carbon composite during the annealing [24]. Carbon electrodes also present the opportunity for a more environmentally friendly approach due to its higher biocompatibility and sustainability when compared to metal electrodes [6]. Although caution is needed when considering other materials that compose the pastes, such as the binders and the solvents, as they can be harmful to humans and/or the environment [5]. We noticed that in screen-printed sensors for water and soil applications over the last 5 years, Ag is the main paste employed in electrodes alongside nondegradable substrates (Table S1 in supporting information).

Another important aspect to consider is the substrate, especially when developing a biodegradable and/or disposable sensor. Common substrates in printed devices include alumina, polyvinyl chloride (PVC), and polyethylene terephthalate (PET) [5,25,26]. The flexibility of the substrate can also be an advantage in many fields, as it opens the possibility of conformable sensors. In the context of environmental monitoring, flexible sensors can be attached to the non-planar surfaces of marine animals or underwater robots, allowing for a less intrusive, more effective biologging monitoring [27,28]. Furthermore, to reduce the cost and environmental impact of electronic devices the use of eco-friendly and sustainable materials that can be reused or naturally discarded has become increasingly important [9]. Several natural biopolymers and degradable synthetic polymers, including starch, chitosan, cellulose, polylactide (PLA), and polycaprolactone (PCL), etc., have shown promise for application in a variety of flexible green electronic devices [9]. More recently, bioderived and biodegradable polyhydroxyalkanoate (PHA) polyesters, including polyhydroxybutyrate (PHB) and its copolymers with polyhydroxyvalerate (PHV) have been recognized for their far-reaching applications, including single use, disposable plastics, and packaging, as well as temporary *in vivo* biomedical technologies [29]. These sustainable and commercially available PHAs can both be produced and broken down, into water and carbon dioxide (CO_2) by living microorganisms in all aerobic and anaerobic environments - features that facilitate the development of biodegradable soil and marine products.

In this paper, we developed flexible and/or eco-friendlier screen-printed electrodes (SPEs) for environmental monitoring applications. The newly prepared graphite-based printed electrodes (G-PEs) were fabricated on biodegradable PHB 92%/PHV 8% (PHB/PHV) substrates produced from renewable feedstocks. To investigate the electrodes chemical and mechanical stability in different media, we demonstrated their applicability in tap water and seawater, as seawater is the most abundant aqueous electrolyte present in the environment [30]. To investigate the G-PEs implementation we compared its performances with the commercial paste electrodes, silver SPEs (Ag-SPEs) and carbon SPEs (C-SPEs), which were printed on PVC substrate. The flexible printed electrodes are shown in Figure S1a in the supporting information. The cyclic voltammetry (CV) and differential pulsed voltammetry (DPV) studies were used to investigate the redox and non-faradaic reactions occurring at the electrode-analyte interface. A detailed investigation of the electrical and morphological properties of the electrodes under different bending conditions was also conducted. Finally, the physical and chemical degradability of the pastes and the substrates were examined in artificial seawater over a period of 16 weeks and by ultrasonication.

2. Experimental section

2.1. Electrode fabrication

In this work, the commercial silver and carbon electrode pastes were screen printed on flexible PVC substrates while the graphite-based carbon paste electrode was printed on PHB/PHV (GoodFellow, 25 μm thickness). In this way, the degradable electrode could be compared with the standard electrodes, which usually employ commercial pastes and a non-degradable plastic substrate. The G-PE was printed using a stencil mask due to the hydrophilic nature of the paste, as in screen printing, the commonly employed stainless steel stencils are sensitive to water. A 20 × 3 mm strip design was used for all studies. The Ag-SPEs were screen printed using a low-temperature curable Ag paste (DuPont, 25 mΩ/sq at 25 μm thickness). For the C-SPEs, a conductive carbon paste (SunChemical, 21 Ω/sq at 25 μm thickness) was used. For the G-PEs, a graphite-based paste was prepared by mixing 8 g of graphite flakes with commercially available polyvinyl alcohol (PVA) based glue (7.5 g) and water (6.7 g). After printing, the Ag-SPEs were dried at 80 °C for 10 min and the C-SPEs at 80 °C for 20 min. The G-PEs had the same drying conditions as the C-SPEs. Finally, the Cu wires were attached on the contact pads. For the Ag-SPEs, commercial Ag ink was used to glue the Cu wire on the electrode at room temperature, while the C-SPEs and G-PEs used the SunChemical carbon paste cured at 80 °C for 20 min to minimize material interference.

2.2. Material characterization

To evaluate the electrical characteristics of the printed electrodes, current–voltage (I-V) measurements were carried out between two voltage probes at distances of 5, 10, 15 and 20 mm for three different strips of the same material using the Omni probe station. As the printed electrodes had the same geometry, the transfer length method (TLM) was applied to obtain the sheet resistance of the screen-printed materials as described elsewhere [31]. The surface thickness of each printed electrode was investigated using a profilometer (Bruker DektakXT) with a scan range of 524 μm using the hills and valleys profile.

A Savitzky–Golay filter using 1000 points was applied to the data to estimate the thickness of the samples. The morphological characterization and the cross-sectional view of the film before and after 16 weeks in artificial seawater was performed by a scanning electron microscope (SEM, Hitachi SU8240 at 8 kV) and analysed using the ImageJ software. The contact angle was estimated by using 10 μL volume of water on top the electrodes with magnified photographed images of the drops from the same angle and direction. The contact angle was estimated using an image editor software (GIMP). To check the mechanical strength of the printed electrodes under flexible conditions underwater, the resistance of the electrodes was measured (Agilent 34461A Digital Multimeter) under 250 cycles of dynamic bending conditions. The printed electrodes were connected to two linear stage motors (from Micronix USA) and both motors were synchronized through a LabVIEW program to move along opposite directions. This motor movements leads to a cyclic bending of the electrodes at bending radius of 20° (Figure S1b,c). The relative resistance change ($\Delta R/R_0$) was calculated by finding the local maxima/minima (R_M) during the cyclic bending and subtracting and dividing each data point by the first resistance point (R_0). This was then multiplied by 100 to find the percentual change, with $\Delta R/R_0 = 100 \times [R_M - R_0]/R_0$. The relative resistance change (ΔR_C) was calculated by subtracting the average of the last 10 points the measurement (mean(R_F)) to the average of the first 10 points (mean(R_I)) and diving it by R_0. This was then multiplied by 100 to find the relative percentage change. Therefore, $\Delta R_c = 100 \times [mean(R_F) - mean(R_I)]/R_0$. The G-PE material long-term stability in artifical seawater (10 days) was measured by monitoring the resistance of the electrode with a digital multimeter (Agilent 34461A) through a LabVIEW controlled programme (experimental setup shown in Figure S1e).

2.3. Electrochemical setup

The CV and DPV electrochemical analysis of the printed electrodes were carried out using the Metrohm Autolab (PGSTAT302N). A 3-electrode system, with a commercial Ag/AgCl RE, a platinum counter electrode and a printed (Ag-SPE, C-SPE or G-PE) or standard (glassy-carbon electrode, GCE) WE, were employed in the CV and DPV studies (experimental setup shown in Figure S1d). For electrochemical measurements all reagents were used as received and all solutions were prepared in deionized (DI) water unless otherwise mentioned. Tap water was taken from the laboratory tap and immediately tested. An artificial seawater solution was prepared by mixing 38 mg/mL of unrefined sea salts in DI water. 50 mM of Potassium hexacyanoferrate(II) trihydrate (FeCN, Sigma) was solubilized in 0.1 M $NaNO_3$. The experiments were performed under normal ambient conditions except for the ferrocyanide studies, which were done both in ambient and nitrogen atmosphere. Ferrocyanide (FeCN) was used to compare the voltammetric behavior of the SPEs in contrast to a standard GCE. The CV and DPV static bending studies were performed by attaching the electrodes to 3D printed probes of 1.60, 1.25, 1.00, and 0.80 cm radius. The same electrode was used throughout the bending experiment. For the 10-day long-term CV and DPV study, the electrodes were left in artificial seawater and the electrochemical voltammograms were measured on days 1, 4, and 10. For the sensor application studies, the electrodes were modified with 10 uL of 50 mg/mL graphene oxide (GOx, Graphene Supermarket) to test for nitrite (NO_2^-) sensing. The GOx was drop casted on top of the electrodes and dried at 80 °C for 10 min. The GOx was not optimised for sensing performance, and it was diluted without further treatment. The electrodes were tested with 3 mM of $NaNO_2^-$ in artificial seawater. A carbon pasted was added to the top of the Ag-SPE, as most sensors use carbon paste for the WE. Only the part covered with the carbon paste was submerged in the solution. The paste was dried using the same methods as in Section 2.1. The WE had an active area of 10 × 3 mm for all electrodes.

2.4. Physical and chemical degradability studies

The degradability studies were conducted by placing the printed electrodes for 16-weeks in artificial seawater at 37 °C in a CO_2 incubator (Thermo Scientific HERAEUS BB 15). Optical images of the G-PE before and after 16 weeks at 37 °C in artificial seawater were taken using a Nikon Eclipse LV100ND microscope connected with Leica MC170HD camera. For the ultrasound disintegration studies, the CamLab camSonix C575T ultrasonic bath was used at room temperature. The electrodes with and without the substrate, and the PHB/PHV substrate were sonicated in artificial seawater with varying times.

3. Results and discussion

3.1. Material characterization

The sheet resistances (R_S) of the SPEs were calculated using TLM as given in Fig. 1a-1c and the profilometry analysis of the electrodes can be seen in Figure S2. The analysis reveals that the G-PE (R_s = 30.1 Ω/sq) and the C-SPE (R_s = 26.9 Ω/sq) have almost similar values which are much higher than the one for the Ag-SPE (R_s = 0.053 Ω/sq). To study the paste topography and thickness, the surface profilometry analysis (shown in Figure S2) was carried out and it shows that the G-PE presented the largest variation in electrode thickness (20–53 μm), compared to the C-SPEs (9–15 μm) and Ag-SPEs (7–12 μm). The G-PEs were about 10% less conductive than the C-SPEs, however the conductivity of the sustainable paste can be improved by using carbon additives such as graphene or CNTs [20,32]. As the conductivity of the G-PE is in the range of the C-SPEs, it should produce an adequate performance for preliminary studies. Furthermore, we also compared the observed R_S values of Ag-SPE and C-SPE with commercial values (given in Table S2). The measured R_S of Ag-SPEs is twice that of the commercial value while the measured R_S for the C-SPEs was 1.3 times greater than the reported commercial R_S. For both SPEs, the thickness was one third or less short of 25 μm, which partially explains the difference between the measured and commercial R_S as thinner layers tend to have a higher R_S [33]. Difference in curing temperatures and processing times might also influence the results, as well as the material composition.

The contact angle analysis showed that the sustainable graphite-based paste is more hydrophilic than the commercial pastes. The angle between the water droplet and the G-PE was of 40°, while for the Ag-SPE and the C-SPE was 156° and 70°, respectively (Fig. 1d-1f). A more hydrophilic conductive path improves the performance of electrodes in water-quality monitoring, as wettability has been shown to increase the charge transfer rate between the electrode and the electrolyte [34]. To check the adhesion and delamination of the printed layer from the substrate, cyclic bending measurements were performed. This only provides information about the mechanical properties of the electrodes during the bending cycles. Fig. 1g-1i shows the measured resistance before and after cyclic bending and during the 250 bending cycles. The C-SPE showed a very stable response during bending and quickly returned to almost the same resistance it had initially, with a relative resistance change (ΔR_C) of 2.3% (after the 250 bending cycles), while for the Ag-SPE and the G-PE the values were 32.2% and 47.3%, respectively. All electrodes resistance varied considerably during cyclic bending from the planar to the bending position (Figure S3) with the G-PE having the largest $\Delta R/R_0$ variation (from −7.7% to 61.0%) and the C-SPE, the lowest (from 2.5% to 35.5%), and the Ag-SPE, a $\Delta R/R_0$ variation of about 14.5% to 77.0%. This large resistance variation and steady increase of $\Delta R/R_0$ during bending for the G-PE and the Ag-SPE could indicate a breakage in the paste composite when bending. A more structural analysis needs to be carried out to understand the cracking of the bulk of material. This change is permanent as the resistance after cyclic bending did not return to

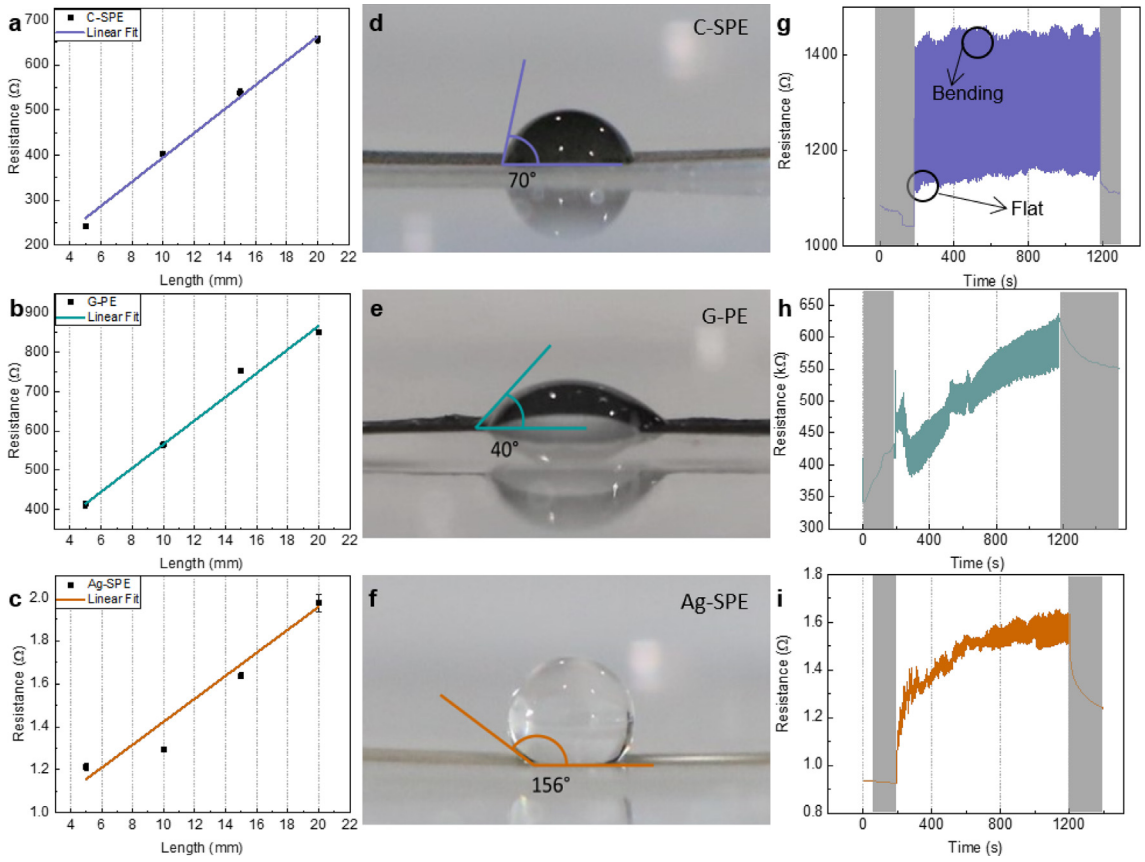

Fig. 1. C-SPE, G-PE, and Ag-SPE: (a-c) Transfer length method for the determination of the sheet resistance. (d-f) Contact angle measurement between the electrodes and a water droplet. (g-i) Resistance monitoring before and after cyclic bending (grey rectangles) and during cyclic bending of the electrodes.

the initial values. Even though the Ag-SPE showed a high variation in resistance, it also presented the lowest overall resistance in the Ω range while the carbon-based electrodes had resistances in the kΩ range.

Fig. 2 shows the surface morphology (Fig. 2a-2f) and the cross-sectional view (Fig. 2g-2 l) of the C-SPEs, G-PEs and Ag-SPEs. The porous microstructures of the C-SPEs (Fig. 2a, 2d) and Ag-SPEs (Fig. 2c, 2f) remains unaffected even after 16 weeks in artificial seawater while a clear difference can be seen in the before and after SEM images of the G-PE (Fig. 2b, 2e), where a higher porosity is observed likely due to material degradation. From the images, one of the reasons for the higher mechanical stability of the Ag- and C-SPEs could be attributed to the fine-grained packed structure compared to the amorphous like stacked layers observed in the graphite electrode. Furthermore, the number of active sites which are capable of ionic reactions largely depends on the microstructure and crystallinity of the electrode. In this way, the fine-grained compact structure of the Ag-SPE is expected to have a less active area as compared to the loosely disordered structure of carbon flakes, but a higher mechanical stability. The film morphologies are distinct for each electrode material, with a striking difference between the two carbon-based pastes. While the C-SPEs showed a spherical nanostructure in the sub-100 nm range, the G-PEs showed stacked, smooth graphite flakes, likely due to the combination of different carbon materials, binders and solvents used in the paste preparation. The cross-sectional view of the electrodes (shown in Fig. 2g-2 l) shows that the films are firmly adherent to the substrate except for the G-PE after 16 weeks in artificial seawater (Fig. 2k), indicating that the paste is starting to detach from the substrate. The thickness of each film was measured from the cross-section view (4.7–10.5 μm for the Ag-SPE and 7–18.6 μm for the C-SPEs) without much change in thickness before and after 16 weeks in artificial seawater. The G-PEs, however, presented a wide range in paste thickness, from 40 to 61 μm and 49.5–87 μm before and after 16 weeks in artificial seawater, indicating paste degradation. These results are similar to the profilometer ones (Table S2). Another parameter that should be taken into consideration is PVA degradation. PVA is a water-soluble polymer and has been shown to accelerate degradation of polymer mixtures in seawater [35]. Therefore, PVA degradation likely contributes to the change in G-PE paste thickness seem throughout the 16 weeks by facilitating material hydrolysis.

3.2. Electrochemical analysis

The CV and DPV analysis for the GCE, C-SPE, G-PE, and the Ag-SPE electrodes in FeCN were carried out and the curves are shown in Fig. 3a and 3b. These electrochemical analyses show that each electrode exhibits a slightly different cyclic behaviour due to their unique material composition involved in the electrochemical reaction. The C-SPE exhibits a similar current density when compared to the standard GCE. However, the Ag-SPE current density is 3 times higher than that of the carbon electrodes when comparing the current density for the FeCN oxidation peak (j_{FeCN}). Considering the difference in sheet resistance from the I-V sweep measurement (from Fig. 1a to 1c) and that silver is generally more conductive than carbon, this is an expected result. Electrode materials need a fairly high electronic conductivity so the rate-limiting process will not the be the electrons moving through the material but the electron movement across the electrode/-solution interface [36]. Nonetheless, the electrode intrinsic conductivity can be one of the factors that affects the current performance. As the electrodes have different electrical resistances which in turns affects the j_{FeCN}, each printed electrode j_{FeCN} was adjusted to that of

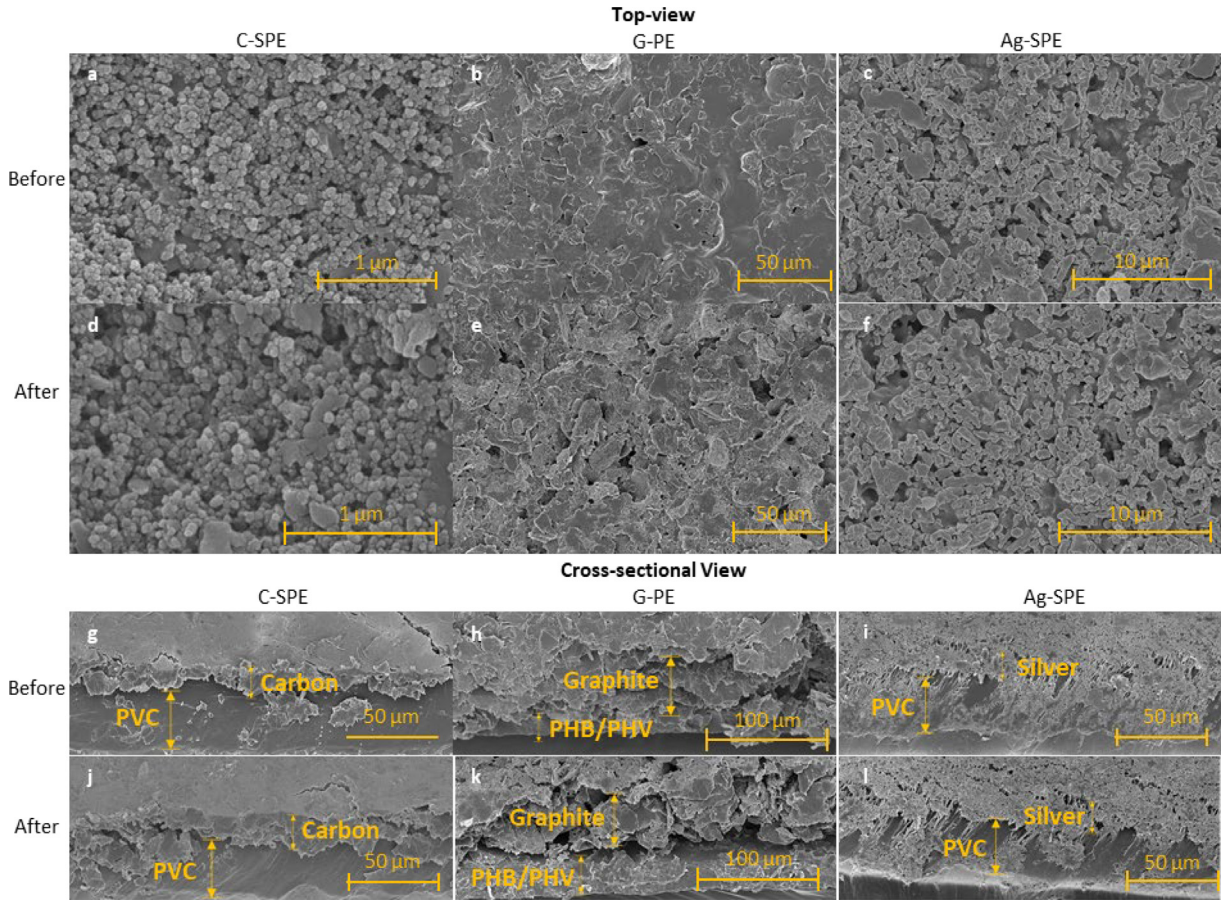

Fig. 2. Top and cross-sectional SEM images of C-SPE, G-PE, and Ag-SPE (left to right). Surface morphology of the electrode pastes before (a-c) and after 16 weeks in artificial seawater (d-f). Cross-sectional view of the electrode pastes before (g-i) and after 16 weeks in artificial seawater (j-l).

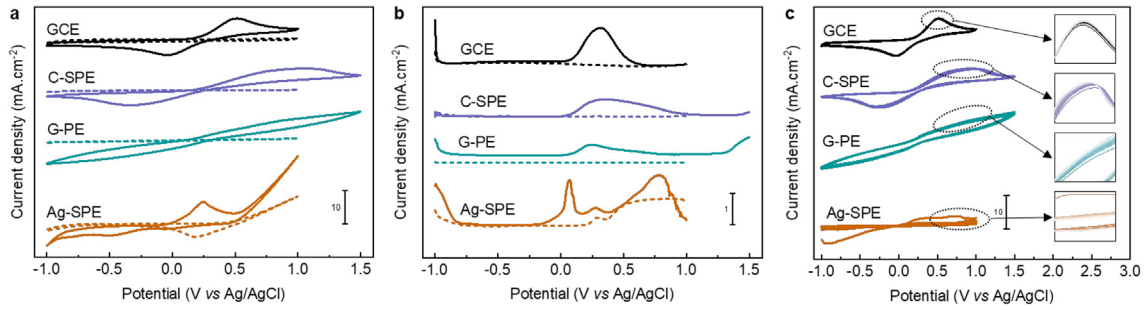

Fig. 3. GCE, C-SPE, G-PE, and Ag-SPE (top to bottom) CVs (a) and DPVs (b) for 50 mM FeCN in 0.1 M $NaNO_3$ with a scan rate of 100 mV/s (full line) and 0.1 M $NaNO_3$ blank (dashed line) under ambient condition. (c) CVs of 50 mM FeCN in 0.1 M $NaNO_3$ for the different electrodes over 15 continuous cycles under ambient condition and magnified FeCN redox peaks. The scale bar applies to all electrodes in the same voltammogram.

the standard GCE for a better comparison between the voltammograms. The current densities before the correction were calculated by their active area, which is 1 × 0.3 cm for the printed electrodes and the circular area for the 3 mm diameter GCE. The correction factor was calculated by dividing the printed electrode FeCN oxidation peak current densities, PE-j_{FeCN}, by the respective GCE oxidation peak current densities, GCE-j_{FeCN}. Therefore, the Ag-SPEs had their current densities divided by a correction factor of 3.40, the C-SPEs by 0.90 and the G-PEs by 0.14 which was later used for the CVs and DPVs unless stated otherwise.

When correlating with the measured R_S (Table S2), the more conductive electrode presented the higher oxidation current but not on the same proportions. This could be due to how the electrodes react with the analyte and the supporting electrolyte solution (such as the oxidation of silver) as electrode conductivity is not the only parameter that affects the electrode performance [30]. The C-SPE showed clear peaks in both voltammograms, although broader than the GCE ones while the G-PE did not present clear peaks in the CV however did have a peak in the DPV. As the G-PE did not show a reliable peak, the correction factor was not used throughout this paper. The Ag-SPE can react with the FeCN to form a new salt complex which explain the appearance of other peaks in the Ag-SPE voltammograms [37], explaining why only the first few cycles show a clear oxidation peak. This can be better seen in Fig. 3c, where the electrodes were cycled

15 times in 50 mM FeCN. While the carbon electrodes appear to be quite stable, the Ag-SPE current density decrease sharply after the first cycle due to the reaction of Ag with FeCN.

The variation of the CV redox peak intensities in air was compared in Fig. 4a. The current density was not adjusted for Fig. 4. It was noted that the redox peak intensity changed with the cycles and the change of j_{FeCN} per cycle can be seen in Fig. 4b. The Ag-SPE presented the expected results of a sharp decreasing trend however the carbon electrodes current density increased with each cycle. Comparing the first and last cycle, there was an increase of 2.0, 3.1 and 8.8% for the GCE, C-SPE and G-PE respectively and a sharp decrease of −81.8% for the Ag-SPE. This is not what usually happens and to further investigate how the atmosphere affects the electrodes, the CV studies with 50 mM FeCN were repeated under an inert N_2 atmosphere (Fig. 4c and Fig. 4d). The electrodes were also cycled 15 times and the results can be seen in Figure S4.

Interestingly, although there was a clear shift to the left in the peaks for the carbon printed electrodes in Fig. 4a, the G-PE redox peaks dramatically increased under inert atmosphere, being now comparable to the C-SPE voltammogram, while the C-SPE showed only a slight increase in current density when compared to the normal atmosphere results. This difference in j_{FeCN} for the G-PEs under different

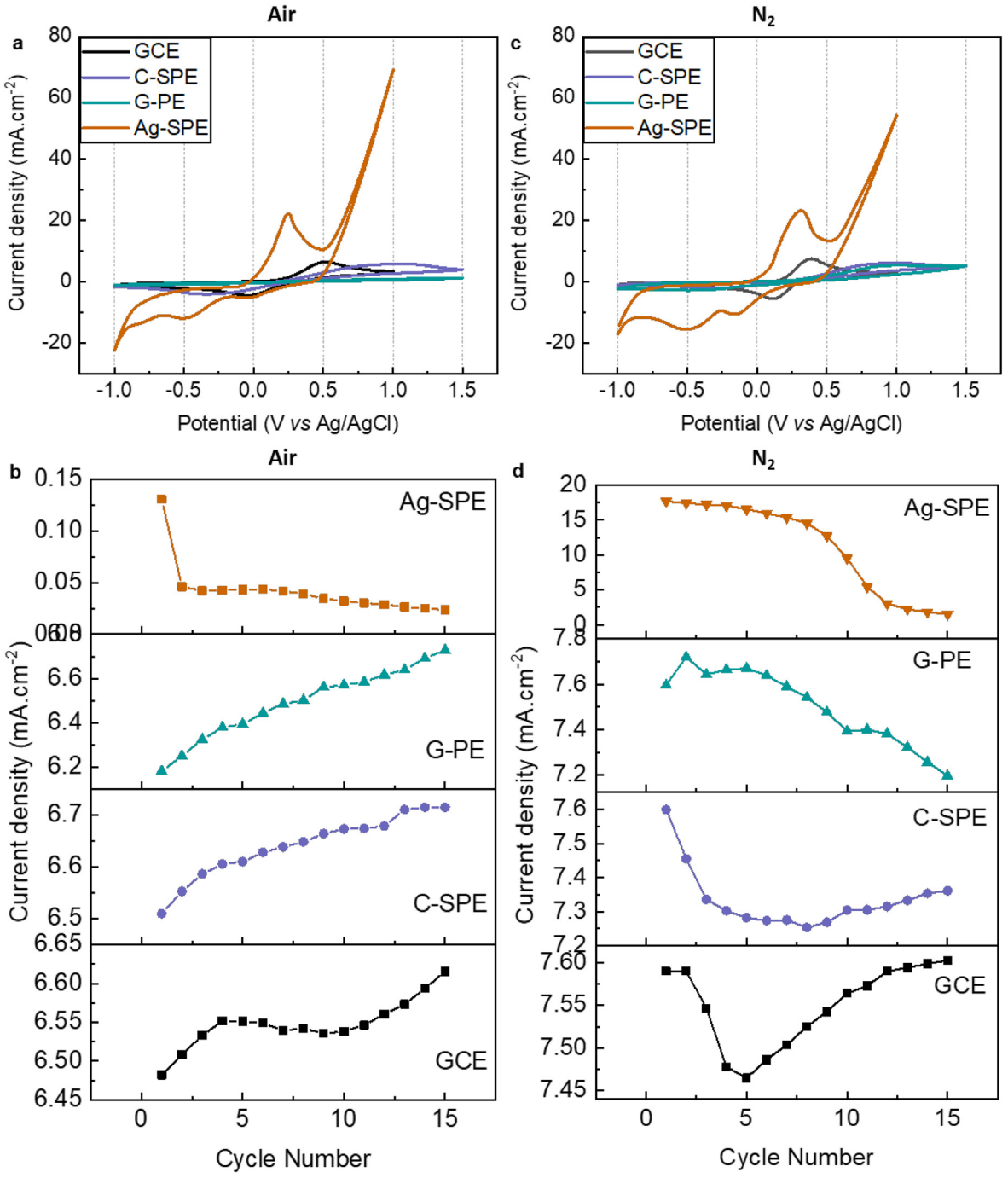

Fig. 4. (a) Comparison of the CV of the printed electrodes in air atmosphere. (b) The FeCN peak current density variation of individual electrodes during 15 cycles in air atmosphere. (c) Comparison of the CV of the printed electrodes in N_2 atmosphere. (d) The FeCN peak current density variation of individual electrodes during 15 cycles in N_2 atmosphere.

atmospheres could indicate some adjustment issues between the manually printed electrodes, which is to be expected when compared to the SPEs. For example, as the G-PEs presented the largest variation in electrode thickness (Figure S2), this could influence the paste properties. A more uniform printing can decrease this difference in Faradaic current. The decrease in the Ag-SPE current density can be seen more clearly in this case. More importantly, the increase in j_{FeCN} with each cycle for the carbon electrodes did not appear to occur under an inert atmosphere (Fig. 4c,4d). This time, when comparing the first and last cycle, the GCE electrode was mostly stable (increase of 0.2%) while the C-SPE, the G-PE and the Ag-SPE presented a decrease of 3.1, 5.3 and 91.5% respectively. This could indicate that gases present in the atmosphere could be reacting with the carbon electrode surface, however further studies are needed to confirm this behaviour. To investigate the electrodes performance in water quality monitoring, we conducted further electrochemical studies in artificial seawater and tap water as discussed below.

3.3. Interaction with seawater and tap water

The printed electrodes were also tested in tap water and artificial seawater and compared to the standard GCE (Fig. 5). In tap water (Fig. 5a,5b), the GCE seems to be the most stable electrode, presenting no redox peaks in the CV and a flat background in the DPV. The printed electrodes instead display some response, with the C-SPE showing a clearer oxidation peak and the Ag-SPE a larger anodic current density. This could once more indicate that the binders used in the C-SPEs influence the voltammogram response. However, the current densities are in the microampere range, which is quite low when compared to the artificial seawater voltammograms (Fig. 5c,5d). When considering the EU's Water Directive 98/83/EC maximum permitted concentration of Cl^- and SO_4^{2-} of 200 mg/L (7.05 mM) and 250 mg/L (2.60 mM) respectively [38], the current density seems reasonable, as the presence of ions is much lower than in other solutions. The G-PE did not display any reaction to the elements present in tap water. As the difference between the silver and carbon electrodes was not as significant, both could be employed as electrodes in mediums with low ionic strength such as tap water. Naturally, it is important to keep in mind silver's tendency to oxidize. In artificial seawater, the electrodes responses were quite different (Fig. 5c,5d) and followed the expected trend as Ag is known to interact with chloride and sulphate ions [16,17]. The Ag-SPE presented a clear redox peak for both CV and DPV while the carbon electrodes showed little to no response. This indicates that the carbon-based electrodes are more suitable for applications in solutions with high ionic strength, especially when considering the Ag interaction with the halide family.

3.4. Static bending study

The printed electrodes were studied under no bending and static bending of 1.60, 1.25, 1.00, and 0.80 cm radius in artificial seawater (Fig. 6). In Fig. 6a and 6b, The Ag-SPE presented a slight increase of current density at the first bending radius of 1.60 cm followed by a steady decrease. The conductivity of the Ag-SPE could have

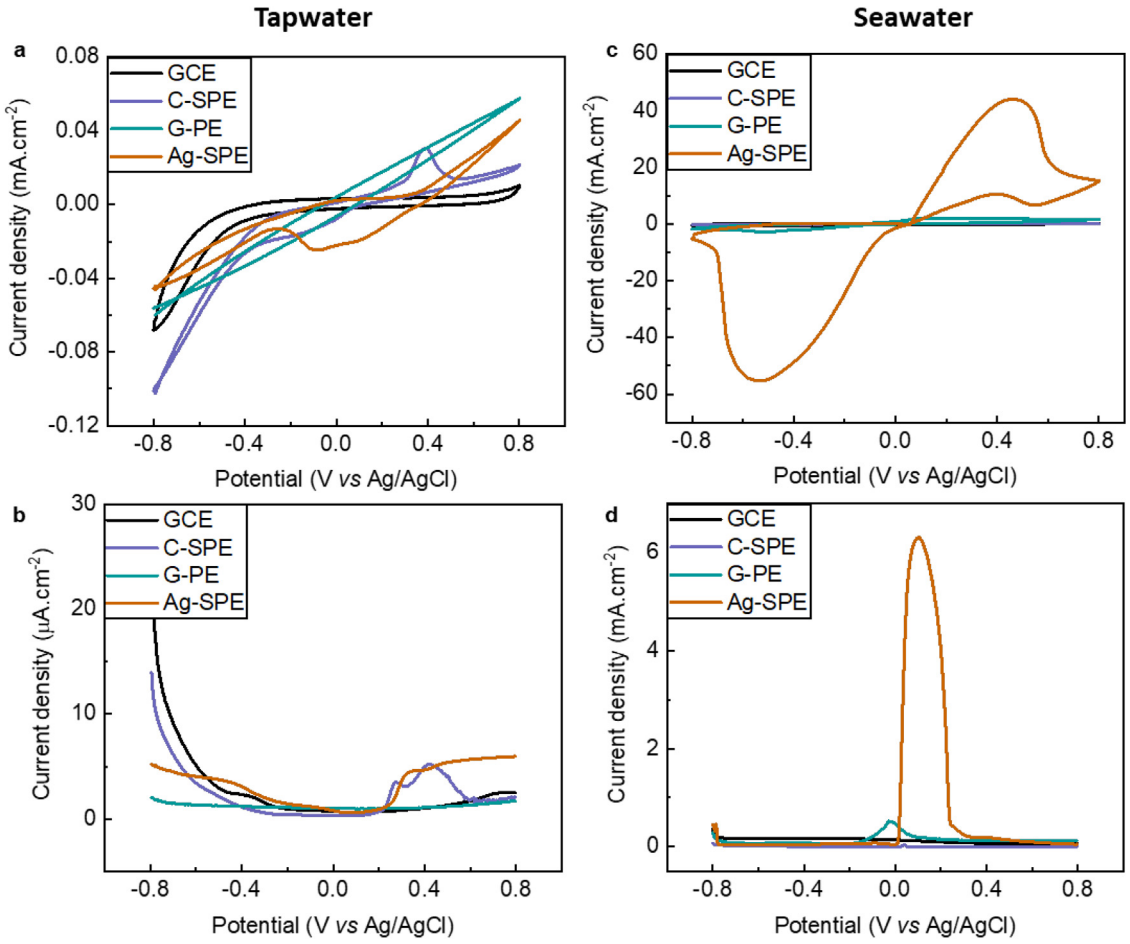

Fig. 5. (a) and (b) Comparison of CV and DPV curves for the GCE, C-SPE, Ag-SPE and G-PE in tap water. (c) and (d) Comparison of CV and DPV curves for the GCE, C-SPE, Ag-SPE and G-PE in sea water.

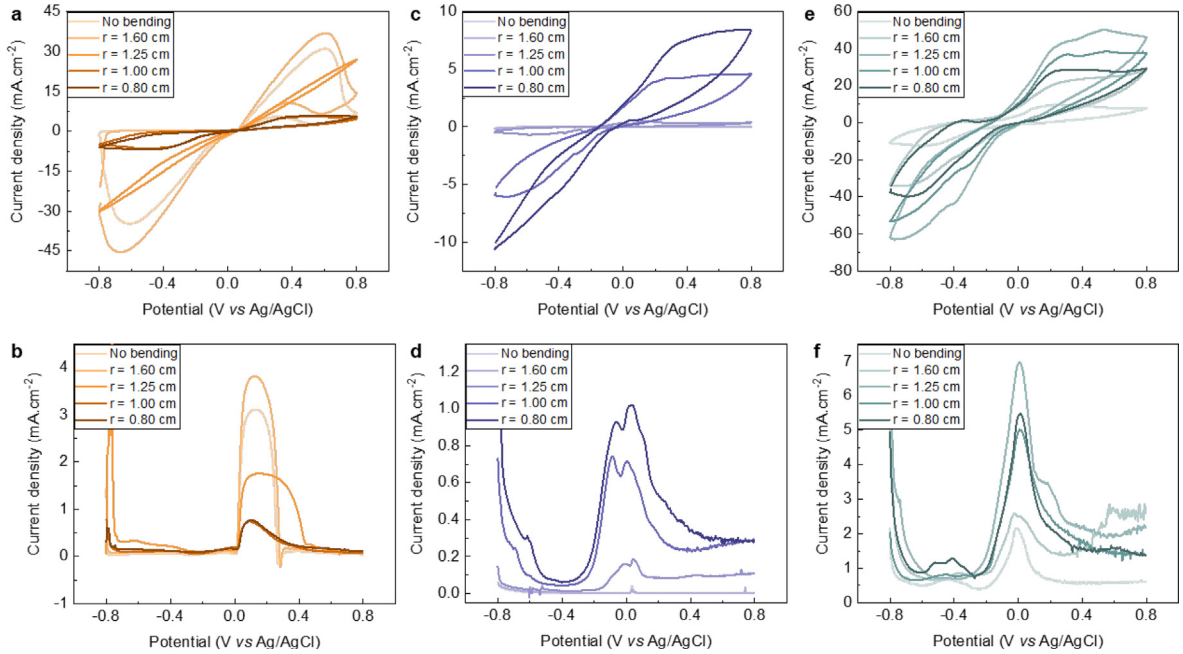

Fig. 6. Static bending CVs (top) and DPVs (bottom) of Ag-SPE (a and b), C-SPE (c and d), and G-PE (e and f) under no bending, and bending at 1.60, 1.25, 1.00, and 0.80 cm radius in artificial seawater.

decreased due to material deterioration from analyte interaction or introduction of defects from bending conditions. The C-SPE (Fig. 6c,6d) current density increased while the electrodes were bent. From the cyclic bending experiments (Fig. 1g), the C-SPE presented the most stable response under bending. Bending under normal atmosphere seems to increase the electrode current response likely due to its mechanical stability and surface reaction with atmospheric gases, as seen in Fig. 4b. The G-PE (Fig. 6e,6f) had a similar trend up until a radius of 1.25 cm, where then the current density started to decrease, possibly due to material degradation or cracking. A table summarizing the CV and DPV current densities peaks according to the no bending state can be seen in Table S2.

3.5. Long-Term study

The G-PE had its resistance monitored over a 10-day period and presented a very high resistance, in the hundreds of kΩ (Figure S5). The resistance shifted to almost 1 MΩ around day 7 and then decreased to 400 kΩ. A probable cause for this large resistance peak is a shift in the material position throughout the days, causing the electrode to bend (as seen previously in Fig. 1h), while other smaller resistance increases could be due to material degradation. The printed electrodes also had their long-term properties studied by analysing their CV and DPV in artificial seawater over a 10-day period (Figure S6). The current density increased over time for all electrodes. This behaviour is similar to what was seen in Fig. 4a under normal atmosphere, again indicating that gases present in the atmosphere could be reacting with the solution and interfering with the experiment stability.

3.6. Nitrite sensing in artificial seawater

To demonstrate the sensing performance of the different pastes, the electrodes were modified with GOx for NO_2^- sensing. GOx and carbon-based materials are known to catalyse NO_2^- into nitrate, with a faradaic reaction at around + 0.8 V, making it a suitable candidate to compare the printed electrodes performances [39]. Fig. 7 shows the CV and DPV of the different electrodes with 0 and 3 mM $NaNO_2^-$. The current densities were not adjusted for the voltammograms in Fig. 7. The GCE showed the best performance (Fig. 7a and 7e), with a sharp redox peak at around + 0.8 V. The Ag-SPEs had a carbon-paste layer to mimic what is usually done for the WE. Even though the carbon layer was present, the Ag layer still interfered with the results, presenting a noisy background in the DPV. However, overall, the result was similar to the one obtained by the C-SPE (Fig. 7c and 7f) and showed a higher current density. The NO_2^- oxidation peak was not as distinguishable for the G-PE (Fig. 7d and 7 h), although a change in current can be clearly seen when comparing with no analyte addition. These results are similar to those obtained in Fig. 3 and indicate that the C-SPE produces similar results to the GCE, while the Ag-SPE is not as suitable for seawater applications. Furthermore, the electron-transfer in the G-PE is not as effective, which compromises the redox peak shape. Further studies are necessary to improve the conductivity so the performance can be increased.

3.7. Physical and chemical degradability studies

In the current work both a biodegradable PHB/PHV plastic substrate and non-toxic G-PE were used as eco-friendly ingredients for disposable electrochemical electrodes to be used for environmental or water quality monitoring devices. To demonstrate the physical and chemical degradability of the SPEs the disintegration and dissolution of the Ag-SPE and C-SPE on PVC substrates and the G-PE on PHB/PHV substrates in artificial seawater solutions was examined. After being immersed in artificial seawater at 37 °C for 16 weeks, the SPEs retained their original weight, indicating no loss of material when left undisturbed. Furthermore, neither the G-PE, nor the PHB/PHV substrate changed significantly (Fig. 8a,8b), retaining ≈82% of its original weight. This may be explained by the material characteristics of the PHB/PHV substrate. Unlike most other currently available biodegradable plastics or polymer substrate materials, PHB and PHB/PHV copolymers are generally water-insoluble and thus, relatively resistant to hydrolytic degradation [40]. The degradation of PHB/PHV copolymers therefore depends greatly on their biological environment and can often require a duration of at least a few months, even years [41,42]. For example, a 50 μm thick PHB/PHV film in soil

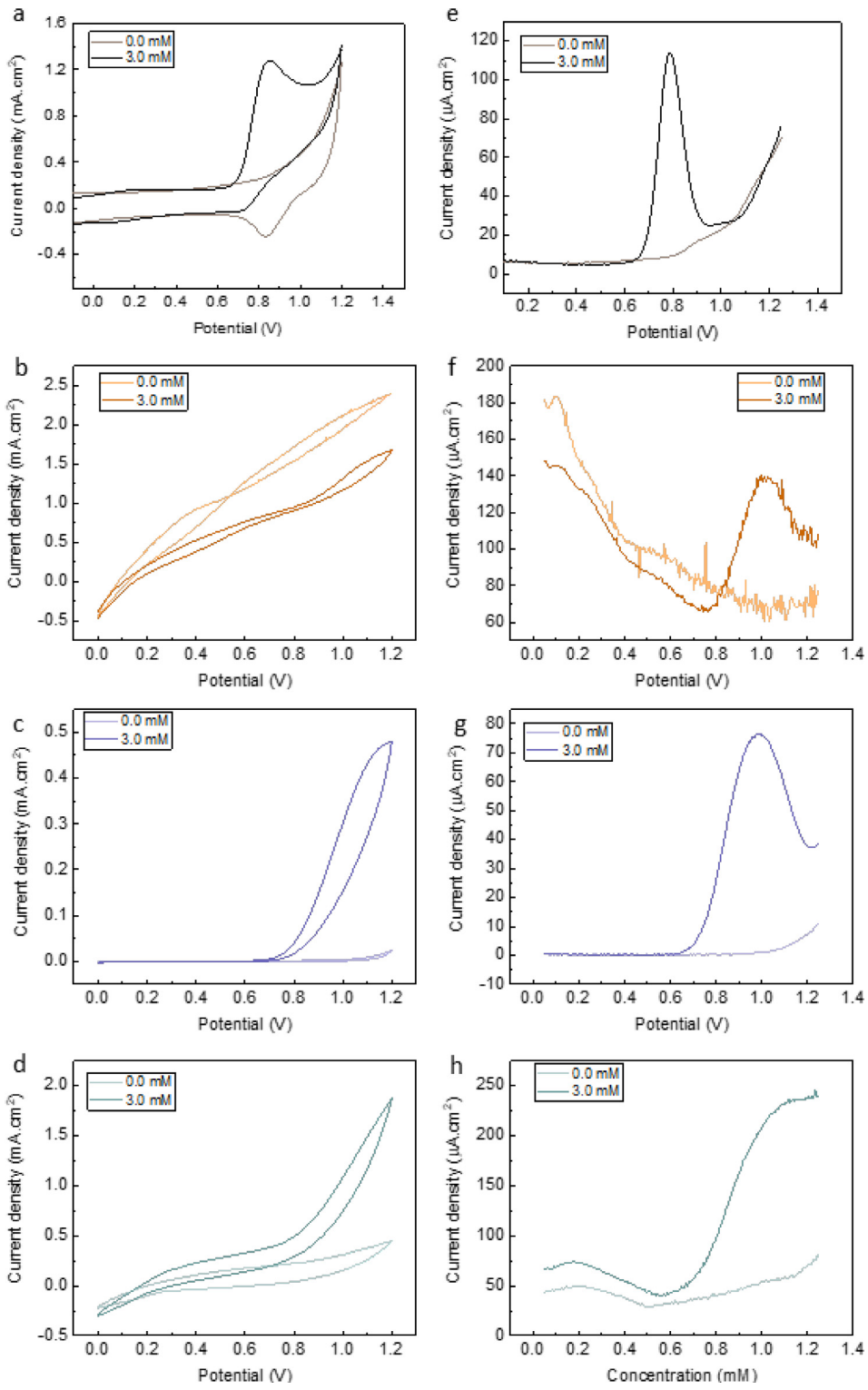

Fig. 7. CV of the (a) GCE, (b) Ag-SPE, (c) C-SPE, and (d) G-PE with 0 and 3 mM $NaNO_2^-$ in artificial seawater. DPV of the (e) GCE, (f) Ag-SPE, (g) C-SPE, and (h) G-PE with 0 and 3 mM $NaNO_2^-$ in artificial seawater.

(25 °C) required ten weeks to completely degrade [43]. In sea water (15 °C), the same film required 50 weeks to achieve complete weight loss. Nevertheless, these microbiologically derived synthetic polymers are compostable susceptible to anaerobic biodegradation in sediments, non-toxic and have good oxygen permeability, making them ideal material choices for short to medium-term environmental monitoring applications [40].

For a timelier disintegration and dissolution of the disposable electrochemical electrode, ultrasound technology, a technique which has proven advantageous in the field of polymer chemistry for yielding degradation, was explored [44]. Despite more than 3 h of sonication, the PHB/PHV substrate remained relatively unchanged. The G-PE, on the other hand, began to dissolve after less than 1 min of sonication. As can be seen in Fig. 8c, after 5 min of sonication the G-PE was almost

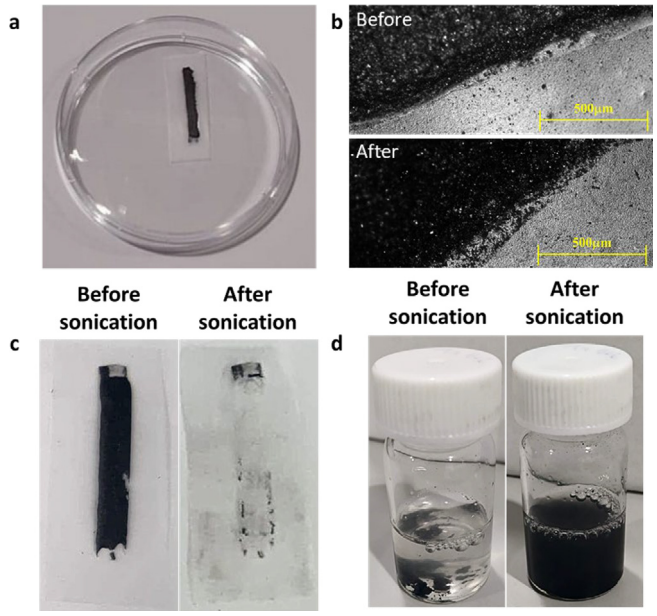

Fig. 8. (a) G-PE on PHB/PHV substrate after 16 weeks in artificial seawater at 37° C, (b) Optical microscope image of G-PE on PHB/PHV substrate before (top) and after (bottom) 16 weeks in artificial seawater at 37° C, (c) G-PE on PHB/PHV substrate before and after 5 min of ultrasound treatment in artificial seawater and (d) Graphite based paste in its cured form, free from substrate before, and after 5 min of ultrasound treatment in artificial seawater.

entirely removed from the PHB/PHV substrate. The degeneration, or lack thereof of substrate materials can also significantly influence the dissolution processes of the conducting traces they support, e.g., due to chemical binding between the substrate and the paste. Considering this, the dissolution of the graphite-based paste in its cured form, free from substrate in artificial seawater was also explored using sonication. As can be seen in Fig. 8d, the G-PE totally dissolved after 5 min of ultrasound treatment. Furthermore, considering the graphite-based paste is composed of only graphite, PVA and water, the byproducts of the degraded species are not as harmful for the environment when comparing with traditional electrodes. It offers advantages over glass and metal-based electrodes particularly if disposable electrodes are needed or when deploying electrodes in areas where there is a risk of breakage or of losing them. However more in-depth and longer studies are still necessary to understand the complete impact of biodegradable substrates and inks, especially when considering the PHA/PHB microplastic byproducts. The degradation and dissolution of the commercial pastes was also examined in artificial seawater. Both the Ag-SPE and C-SPE with (Figure S7a) and without the PVC substrate (Figure S7b) remained unchanged after 5 (with the PVC) and 30 min (without the PVC) of ultrasonication treatment and neither presented any differences before and after 16 weeks in artificial seawater which is in line with the SEM results (Fig. 2). Therefore, the findings of the current study therefore suggest that the G-PE on PHB/PHV substrate presents a promising platform for eco-friendly electrochemical electrodes that may serve as single use or short-term sensing elements for environmental or water quality monitoring applications.

4. Conclusion

In the current work a biodegradable PHB/PHV substrate and a more sustainable G-PE were used as eco-friendly ingredients for disposable electrochemical electrodes to be used for environmental or water quality monitoring devices. An in-depth investigation of how different printed conductive pathways would behave under different bending and electrochemical conditions was conducted. The Ag-SPEs were highly conductive (0.053 Ω/sq) when compared to the C-SPEs (26.9 Ω/sq) and the G-PEs (30.1 Ω/sq), as expected of a metal-based paste. However, under cyclic bending conditions, the Ag-SPE and G-PE $\Delta R/R_0$ varied to more than 60%, while the C-SPE showed a more stable variation of 35.5%. From the electrochemical CV, DPV, and EIS studies, it was observed that the Ag paste easily reacted with the salts present in the solutions while the carbon-based electrodes were mostly inert. The tap water and seawater studies demonstrated that there is almost no difference between the materials in tap water due to the low concentration of ions but in seawater a clear difference in the faradaic current was observed, supporting the findings from previous electrochemical studies that Ag readily reacts with halides [15]. The electrodes were further modified with GOx and tested for NO_2^- detection. While the C-SPE showed sharp peaks, the electron-transfer of the G-PE needs to be further improved.

To demonstrate the physical and chemical degradability of the SPEs the disintegration and dissolution of the G-PE on PHB/PHV substrates in artificial seawater solutions was examined. After being immersed in artificial seawater for 16 weeks at 37 °C, neither the G-PE, nor the PHB/PHV substrate changed significantly due to the relative resistance of the water insoluble substrate to hydrolytic degradation. This indicates the G-PE can withstand up to a few months before being disposed of. Using ultrasound technology, however, the G-PE dissociated from the PHB/PHV substrate in less than 1 min, highlighting the suitability of this eco-friendly electrochemical electrode for single use or short-term water quality monitoring sensors that can be reused or naturally discarded. Meanwhile, the Ag-SPEs and the C-SPEs did not show any degradation or dissolution over the course of 16 weeks in seawater or in the ultrasonication studies.

Overall, we demonstrated the higher electrochemical stability for the carbon-based electrodes and the fabrication of a new, eco-friendlier G-PE for water quality monitoring. Furthermore, although Ag is still the major component in most screen-printed sensors due to its high conductivity, we demonstrated that carbon-based electrodes can be suitable, more sustainable alternatives in highly ionic media. As it stands, the G-PE is better suited to be used as a conductive pathway than as a WE due to its high chemical stability and sheet resistance comparable to available commercial carbon pastes, but low faradaic peak separation. In future studies, we aim to improve the conductivity and charge-transfer capability of the G-PEs and perform further studies in the degradability of the electrodes, focusing on the biodegradability aspect and life-cycle studies.

CRediT authorship contribution statement

Fabiane F. Franco: Conceptualization, Methodology, Data curation, Writing – original draft, Visualization, Investigation, Validation, Writing – review & editing. **Saoirse Dervin:** Writing – original draft, Visualization, Investigation. **Libu Manjakkal:** Writing – original draft, Investigation, Writing – review & editing, Supervision, Project administration.

Declaration of Competing Interest

The authors declare that they have no known competing financial interests or personal relationships that could have appeared to influence the work reported in this paper.

Acknowledgment

This work was supported by the European Commission through the AQUASENSE (H2020-MSCA-ITN-2018-813680) project. The authors thank Dr. Dhayalan Shakthivel for the SEM images and the Bendable Electronics and Sensing Technologies group at the University of Glasgow for offering the laboratory facilities.

Appendix A. Supplementary data

The following files are available free of charge. Electrodes and experimental setup; Cyclic bending $\Delta R/R_0$; Comparison of CVs; Long-term studies; Physical and chemical degradability of Ag-SPEs and C-SPEs; Electrodes electrical and morphological characteristics. (PDF). Supplementary data to this article can be found online at https://doi.org/10.1016/j.jelechem.2022.116592.

References

[1] H. Beitollahi, S.Z. Mohammadi, M. Safaei, S. Tajik, Applications of electrochemical sensors and biosensors based on modified screen-printed electrodes: a review, Anal. Methods 12 (2020) 1547–1560, https://doi.org/10.1039/C9AY02598G.

[2] L. Manjakkal, S. Dervin, R. Dahiya, Flexible potentiometric pH sensors for wearable systems, RSC Adv. 10 (2020) 8594–8617, https://doi.org/10.1039/D0RA00016G.

[3] M. Li, D.-W. Li, G. Xiu, Y.-T. Long, Applications of screen-printed electrodes in current environmental analysis, Curr. Opin. Electrochem. 3 (2017) 137–143, https://doi.org/10.1016/j.coelec.2017.08.016.

[4] F. Wang, Y.-T. Wang, H. Yu, J.-X. Chen, B.-B. Gao, J.-P. Lang, One unique 1D silver (I)-bromide-thiol coordination polymer used for highly efficient chemiresistive sensing of ammonia and amines in water, Inorg. Chem. 55 (2016) 9417–9423, https://doi.org/10.1021/acs.inorgchem.6b01688.

[5] J. Kim, R. Kumar, A.J. Bandodkar, J. Wang, Advanced materials for printed wearable electrochemical devices: A review, Adv. Electron. Mater. 3 (2017) 1600260, https://doi.org/10.1002/aelm.201600260.

[6] A. Ahamed, L. Ge, K. Zhao, A. Veksha, J. Bobacka, G. Lisak, Environmental footprint of voltammetric sensors based on screen-printed electrodes: An assessment towards "green" sensor manufacturing, Chemosphere 278 (2021), https://doi.org/10.1016/j.chemosphere.2021.130462 130462.

[7] Y. Chen, Y. Zilberman, P. Mostafalu, S.R. Sonkusale, Paper based platform for colorimetric sensing of dissolved NH3 and CO2, Biosens. Bioelectron. 67 (2015) 477–484.

[8] Y. Li, W. Chen, L. Lu, Wearable and biodegradable sensors for human health monitoring, ACS Applied Bio Materials. 4 (2021) 122–139, https://doi.org/10.1021/acsabm.0c00859.

[9] E.S. Hosseini, S. Dervin, P. Ganguly, R. Dahiya, Biodegradable materials for sustainable health monitoring devices, ACS Applied Bio Materials. 4 (2021) 163–194, https://doi.org/10.1021/acsabm.0c01139.

[10] S. Tajik, H. Beitollahi, F.G. Nejad, M. Safaei, K. Zhang, Q. Van Le, R.S. Varma, H.W. Jang, M. Shokouhimehr, Developments and applications of nanomaterial-based carbon paste electrodes, RSC Adv. 10 (2020) 21561–21581, https://doi.org/10.1039/D0RA03672B.

[11] W. Wu, Inorganic nanomaterials for printed electronics: a review, Nanoscale. 9 (2017) 7342–7372, https://doi.org/10.1039/C7NR01604B.

[12] L. Manjakkal, D. Szwagierczak, R. Dahiya, Metal oxides based electrochemical pH sensors: Current progress and future perspectives, Prog. Mater Sci. 109 (2020), https://doi.org/10.1016/j.pmatsci.2019.100635 100635.

[13] M. Li, Y.-T. Li, D.-W. Li, Y.-T. Long, Recent developments and applications of screen-printed electrodes in environmental assays—A review, Anal. Chim. Acta 734 (2012) 31–44, https://doi.org/10.1016/j.aca.2012.05.018.

[14] R. Zhang, S. Xu, Y. Zhu, J. Luo, X. Liu, D. Tang, One-pot facile preparation of Ag nanoparticles for chloride ion sensing, Colloid and Polymer, Science 294 (2016) 1643–1649, https://doi.org/10.1007/s00396-016-3928-1.

[15] J. Bujes-Garrido, D. Izquierdo-Bote, A. Heras, A. Colina, M.J. Arcos-Martínez, Determination of halides using Ag nanoparticles-modified disposable electrodes. A first approach to a wearable sensor for quantification of chloride ions, Analytica Chimica Acta. 1012 (2018) 42–48, https://doi.org/10.1016/j.aca.2018.01.063.

[16] H.S. Toh, C. Batchelor-McAuley, K. Tschulik, R.G. Compton, Electrochemical detection of chloride levels in sweat using silver nanoparticles: a basis for the preliminary screening for cystic fibrosis, Analyst. 138 (2013) 4292–4297, https://doi.org/10.1039/C3AN00843F.

[17] M. Komoda, I. Shitanda, Y. Hoshi, M. Itagaki, Instantaneously usable screen-printed silver/silver sulfate reference electrode with long-term stability, Electrochem. Commun. 103 (2019) 133–137, https://doi.org/10.1016/j.elecom.2019.05.019.

[18] D.G. Gromadskyi, Characterization of Ag/Ag2SO4 system as reference electrode for in-situ electrochemical studies of advanced aqueous supercapacitors, J. Chem. Sci. 128 (2016) 1011–1017, https://doi.org/10.1007/s12039-016-1084-2.

[19] J. Wang, B. Tian, V.B. Nascimento, L. Angnes, Performance of screen-printed carbon electrodes fabricated from different carbon inks, Electrochim. Acta 43 (1998) 3459–3465, https://doi.org/10.1016/S0013-4686(98)00092-9.

[20] J. Wang, M. Musameh, Carbon nanotube screen-printed electrochemical sensors, Analyst. 129 (2004) 1–2, https://doi.org/10.1039/B313431H.

[21] A. Abdelhalim, A. Abdellah, G. Scarpa, P. Lugli, Fabrication of carbon nanotube thin films on flexible substrates by spray deposition and transfer printing, Carbon N Y. 61 (2013) 72–79, https://doi.org/10.1016/j.carbon.2013.04.069.

[22] R.L. McCreery, Advanced carbon electrode materials for molecular electrochemistry, Chem. Rev. 108 (2008) 2646–2687, https://doi.org/10.1021/cr068076m.

[23] P. He, J. Cao, H. Ding, C. Liu, J. Neilson, Z. Li, I.A. Kinloch, B. Derby, Screen-printing of a highly conductive graphene ink for flexible printed electronics, ACS Appl. Mater. Interfaces 11 (35) (2019) 32225–32234.

[24] Y.H. Hou, M.Q. Zhang, M.Z. Rong, G. Yu, H.M. Zeng, Improvement of conductive network quality in carbon black-filled polymer blends, J. Appl. Polym. Sci. 84 (14) (2002) 2768–2775.

[25] K. Uppuluri, M. Lazouskaya, D. Szwagierczak, K. Zaraska, M. Tamm, Fabrication, potentiometric characterization, and application of screen-printed RuO2 pH electrodes for water quality testing, Sensors. 21 (2021) 5399, https://doi.org/10.3390/s21165399.

[26] Y. Huang, T. Wang, Z. Xu, E. Hughes, F. Qian, M. Lee, Y. Fan, Y. Lei, C. Brückner, B. Li, Real-time in situ monitoring of nitrogen dynamics in wastewater treatment processes using wireless, solid-state, and ion-selective membrane sensors, Environ. Sci. Technol. 53 (2019) 3140–3148, https://doi.org/10.1021/acs.est.8b05928.

[27] A. Kaidarova, M. Marengo, G. Marinaro, N. Geraldi, C.M. Duarte, J. Kosel, Flexible and Biofouling Independent Salinity Sensor, Adv. Mater. Interfaces 5 (2018) 1801110, https://doi.org/10.1002/admi.201801110.

[28] A. Kaidaorva, M. Marengo, G. Marinaro, N.R. Geraldi, R. Wilson, C.M. Duarte, J. Kosel, Flexible, four-electrode conductivity cell for biologging applications, Results in Materials. 1 (2019), https://doi.org/10.1016/j.rinma.2019.100009 100009.

[29] K.W. Meereboer, M. Misra, A.K. Mohanty, Review of recent advances in the biodegradability of polyhydroxyalkanoate (PHA) bioplastics and their composites, Green Chem. 22 (2020) 5519–5558, https://doi.org/10.1039/D0GC01647K.

[30] F. Scholz, A.M. Bond, R.G. Compton, D.A. Fiedler, G. Inzelt, H. Kahlert, Š. Komorsky-Lovrić, H. Lohse, M. Lovrić, F. Marken, A. Neudeck, U. Retter, F. Scholz, Z. Stojek (Eds.), Electroanalytical Methods, Springer Berlin Heidelberg, Berlin, Heidelberg, 2010.

[31] L. Manjakkal, W.T. Navaraj, C.G. Núñez, R. Dahiya, Graphene-graphite polyurethane composite based high-energy density flexible supercapacitors, Adv. Sci. 6 (2019) 1802251, https://doi.org/10.1002/advs.201802251.

[32] S. Goodwin, Z. Coldrick, S. Heeg, B. Grieve, A. Vijayaraghavan, E.W. Hill, Fabrication and electrochemical response of pristine graphene ultramicroelectrodes, Carbon N Y. 177 (2021) 207–215. https://doi.org/10.1016/j.carbon.2021.02.078.

[33] J. Kim, W.J. da Silva, R. Abd, bin Mohd Yusoff, J. Jang, Organic devices based on nickel nanowires transparent electrode, Sci. Rep. 6 (2016) 19813, https://doi.org/10.1038/srep19813.

[34] Q. Zhang, T. Li, J. Liang, N. Wang, X. Kong, J. Wang, H. Qian, Y. Zhou, F. Liu, C. Wei, Y. Zhao, X. Zhang, Highly wettable and metallic NiFe-phosphate/phosphide catalyst synthesized by plasma for highly efficient oxygen evolution reaction, J. Mater. Chem. A 6 (2018) 7509–7516, https://doi.org/10.1039/C8TA01334A.

[35] D. Huang, Z.-D. Hu, Y. Ding, Z.-C. Zhen, B. Lu, J.-H. Ji, G.-X. Wang, Seawater degradable PVA/PCL blends with water-soluble polyvinyl alcohol as degradation accelerator, Polym. Degrad. Stab. 163 (2019) 195–205, https://doi.org/10.1016/j.polymdegradstab.2019.03.011.

[36] P.M.S. Monk, Fundamentals of electroanalytical chemistry, John Wiley & Sons, 2008.

[37] K.Z. Brainina, A.V. Tarasov, M.B. Vidrevich, Silver chloride/ferricyanide-based quasi-reference electrode for potentiometric sensing applications, Chemosensors. 8 (2020) 15.

[38] European Comission, Council Directive 98/83/EC of 3 November 1998 on the quality of water intended for human consumption, Official Journal of the European Communities. (1998).

[39] D. Li, T. Wang, Z. Li, X. Xu, C. Wang, Y. Duan, Application of graphene-based materials for detection of nitrate and nitrite in water—A review, Sensors. 20 (1) (2020) 54.

[40] M.Y. Karidurаganavar, A.A. Kittur, R.R. Kamble, Chapter 1 - Polymer Synthesis and Processing, in: S.G. Kumbar, C.T. Laurencin, M.B.T.-N. and S.B.P. Deng (Eds.), Elsevier, Oxford, 2014: pp. 1–31. https://doi.org/https://doi.org/10.1016/B978-0-12-396983-5.00001-6.

[41] M. Avella, E. Martuscelli, M. Raimo, Review properties of blends and composites based on poly(3-hydroxy)butyrate (PHB) and poly(3-hydroxybutyrate-hydroxyvalerate) (PHBV) copolymers, J. Mater. Sci. 35 (2000) 523–545, https://doi.org/10.1023/A:1004740522751.

[42] A.R. Bagheri, C. Laforsch, A. Greiner, S. Agarwal, Fate of so-called biodegradable polymers in seawater and freshwater, Global Challenges. 1 (2017) 1700048, https://doi.org/10.1002/gch2.201700048.

[43] C.W. Pouton, S. Akhtar, Biosynthetic polyhydroxyalkanoates and their potential in drug delivery, Adv. Drug Deliv. Rev. 18 (1996) 133–162, https://doi.org/10.1016/0169-409X(95)00092-L.

[44] E. von der Esch, M. Lanzinger, A.J. Kohles, C. Schwaferts, J. Weisser, T. Hofmann, K. Glas, M. Elsner, N.P. Ivleva, Simple generation of suspensible secondary microplastic reference particles via ultrasound treatment, Front. Chem. 8 (2020) 169, https://doi.org/10.3389/fchem.2020.00169.